RERIC
www.rericjournal.ait.ac.th

Multi-objective Optimal Power Flow Using Fuzzy Satisfactory Stochastic Optimization

Prakaipetch Muangkhiew* and Keerati Chayakulkheeree*, [1]

ARTICLE INFO

Article history:
Received 31 March 2022
Received in revised form
13 June 2022
Accepted 05 July 2022

Keywords:
Active power loss
Fuzzy satisfactory function
Optimal power flow
Total system cost
Voltage magnitude deviation

ABSTRACT

The optimal power flow (OPF) has been widely used in power system operation and planning of power systems. Recently, many advanced optimization methods have been used to solve the OPF problem with different objectives. However, traditional OPF cannot effectively handle multiple objectives, at the same time. Therefore, the main contribution of this is to propose the fuzzy multi-objective optimal power flow (FMOPF) using the stochastic search optimization technique. In the proposed method, particle swarm optimization (PSO) is used to solve the FMOPF by incorporating to minimizing the objective function's fuzzy satisfaction function, including the total system cost, active power loss, and voltage magnitude deviation. The proposed FMOPF is applied to solve the optimal condition for the IEEE 30-bus test system for verification. The simulation results showed that the proposed FMOPF using the PSO method could potentially and effectively determine the best solution for single-objective OPF compared to existing methods. From the results, the proposed method gave the compromise solution among different objectives in the proposed FMOPF in a fuzzy manner by comparing the results obtained with the existing method under the same system data, and control variables.

1. INTRODUCTION

In power system operation, the optimal operation of system equipment for economic, security, quality of supply, and environmental concern is the most required. The vital tool for power system day-to-day operation and planning is optimal power flow (OPF). The OPF was first introduced by Carpentier [1], to operate cost minimization. Nowadays, the OPF has been constantly developed with several objectives and security constraints including solving methods. The OPF is a complex non-convex optimization problem [2] and [3], for determining the optimal solution of a power system considering security constraints. In the OPF formulation, the best operating condition of the power system is determined depending on the desired objectives, for example, total system cost minimization (TSCM), active power loss minimization (APLM), and voltage magnitude deviation minimization (VMDM). Therefore, the best suitable values of control variables are the outputs of OPF. Meanwhile, the power balance and system operating constraints are needed to be met in the OPF problem [4]. The dependent variable obtained and handled by OPF is the generators' reactive power, voltage magnitudes at load buses, and the MVA flow at each branch [5].

*School of Electrical Engineering, Institute of Engineering, Suranaree University of Technology, Nakhon Ratchasima, Thailand.

[1] Corresponding author:
E-mail: keerati.ch@sut.ac.th

In the past decades, non-deterministic search optimization techniques have been continuously developed to solve complex OPF problems, for example, genetic algorithm (GA) in [6] and tabu search (TS) in [7]. Meanwhile, the recent stochastic optimization methods have also been continuously proposed. The black-hole-based optimization (BHBO) was proposed to solve the OPF problem in [8]. Meanwhile, the authors in [9] used the meta-heuristic algorithm to solve the OPF with SVCs consideration. An enhanced adaptive differential evolution (JADE) with a self-adaptive penalty constraint handling technique (EJADE-SP) is proposed to obtain the OPF problem in [10]. Among the modern stochastic optimization techniques, particle swarm optimization (PSO) is one of the most widely used methods, [11] to [13]. Meanwhile, the improved PSO algorithm, stochastic weight trade-off PSO (SWT-PSO), is applied to solve the OPF problem in [14]. However, due to the complex behavior that difficult to find global solutions for OPF, further development to get a better solution is still beneficial.

Moreover, the practical operation of a power system is commonly included in multiple objectives. The best solution for some objectives may lead to a bad solution for some other objectives. Therefore, the multi-objective OPF has been proposed in several kinds of research [15] to [18]. When the optimization problem has two or more objective functions, the problems are called multi-objective optimization problems (MOOP) [16]. Generally, MOOP must be optimized for more than one objective function at the same time. There are many methods proposed for solving MOOP. The classical approach for solving such problems focuses on aligning multi-objective to a single objective. The MOOP can be defined as conflicting objectives by the Pareto optimal method or a fuzzy method [17] to [20] for extracting the best compromise solution obtained from the Pareto front or fuzzy trade-off. Furthermore, various methods can solve the MOOP. For example, the authors in [21] used Mayfly and Aquila (MA) Optimizer algorithms to solve MOOP considering Pareto front solutions. Also, the multi-objective differential evolution (MDE) solution aims to focus only on the required parts of the Pareto set was proposed in [22] In addition, self-adaptive particle swarm optimization (SPSO)-differential evolution (DE) algorithms [23] and manta ray foraging optimization (MRFO) [24] can solve the problem of MOOP as well. Nevertheless, compromised trade-off among multiple objectives may be preferred by the system operator.

Therefore, this paper proposes the fuzzy multi-objective OPF (FMOPF) that is solved by PSO. In the proposed method, the OPF problem is formulated to MOOP. The objective functions include the TSCM, APLM, and VMDM. Several case studies were conducted with different combinations of the three objectives mentioned above. The standard and modified IEEE 30-bus test systems were used to test the proposed OPF problem formulation using PSO for individual single-objective TSCM, APLM, and VMDM. In addition, the FMOPF for trade-off among TSCM, APLM, and VMDM has also been investigated.

In this paper, the problem formulation is discussed in Section 2. Next, the strategy for objective functions fuzzification is offered in Section 3. Furthermore, the simulation result and discussion are given in Section 4. The conclusion is addressed in Section 5. Finally, the nomenclature is given at the end part.

2. PROBLEM FORMULATION

Mathematically, the OPF problem can be represented as follow:

Minimize
$$\boldsymbol{f}(\mathbf{P_G},|\mathbf{V_G}|,\mathbf{T},\mathbf{X_C}), \quad (1)$$

Subject to:
$$\boldsymbol{g}(\mathbf{P_G},|\mathbf{V_G}|,\mathbf{T},\mathbf{X_C})=0 \quad (2)$$

$$\boldsymbol{h}(\mathbf{P_G},|\mathbf{V_G}|,\mathbf{T},\mathbf{X_C})\le 0 \quad (3)$$

In Equation 1, matrix f represents the set of objective functions that are to be minimized. Meanwhile, matrices g and h, in Equations 2 and 3, are the sets of equality and inequality constraints required. Where PG is the matrix of active power generation excluding slack bus generation as,

$$\mathbf{P_G}=[P_{G2},P_{G3},...,P_{GNG}]_{1\times(NG-1)} \ . \quad (4)$$

|VG| is the matrix of voltage magnitude of generator bus,

$$|\mathbf{V_G}|=[|V_{G1}|,|V_{G2}|...,|V_{GNG}|]_{1\times NG} \ . \quad (5)$$

T is the matrix of transformer tap-changing,

$$\mathbf{T}=[T_1,...,T_{NT}]_{1\times NT} \ . \quad (6)$$

XC is the matrix of SVCs reactance values,

$$\mathbf{X_C}=[X_{C1},...,X_{CNC}]_{1\times NC} \ . \quad (7)$$

2.1 *Objective Function*

In this article, TSCM, APLM, and VMDM objective functions are considered.

2.1.1 *Total system cost minimization (TSCM)*

The TSCM problem can be represented as below:

$$\min TSC(\mathbf{P_G},|\mathbf{V_G}|,\mathbf{T},\mathbf{X_C}), \quad (8)$$

where,

$$TSC(\mathbf{P_G},|\mathbf{V_G}|,\mathbf{T},\mathbf{X_C})=\sum_{i=1}^{NG}(a_i+b_iP_{Gi}+c_iP_{Gi}^2) \ . \quad (9)$$

2.1.2 *Active power loss minimization (APLM)*

The APLM is to reduce the transmission losses as:

$$\min APL(\mathbf{P_G},|\mathbf{V_G}|,\mathbf{T},\mathbf{X_C}), \quad (10)$$

where,

$$APL(\mathbf{P_G},|\mathbf{V_G}|,\mathbf{T},\mathbf{X_C})=\sum_{L=1}^{NTL}g_{L,ij}\left[\mathrm{V}_i^2+\mathrm{V}_j^2-2\mathrm{V}_i\mathrm{V}_j\cos\theta_{ij}\right]. \quad (11)$$

2.1.3 *Voltage magnitude deviation minimization (VMDM)*

The VMDM is to keep the voltage quality of a power system, can be formulated as:

$$\min VMD(\mathbf{P_G},|\mathbf{V_G}|,\mathbf{T},\mathbf{X_C}), \quad (12)$$

where,

$$VMD(\mathbf{P_G},|\mathbf{V_G}|,\mathbf{T},\mathbf{X_C})=\sum_{i=1}^{NL}\left|V_i-V_i^{ref}\right|. \quad (13)$$

V_i^{ref} is generally considered as 1 p.u.

2.1.4 *FMOPF*

The FMOPF problem is simultaneously solved for the optimal solution of TSCM, APLM, and VMDM, based on a fuzzy trade-off concept.

2.2 *System Constraints*

The common OPF constraints including power balance and operation are taken into consideration in the proposed method.

2.2.1 *Power balance constraints*

The power balance constraint can be represented by the Newton-Raphson power flow equations. These constraints are handled by solving the power flow solution. Therefore, a feasible solution can be ensured. In addition, the other dependent variables are obtained from this process. The power balance constraints can be described as:

$$P_{Gi} - P_{Di} = \sum_{j=1}^{NB} \left[G_{ij} |V_i||V_j| \cos(\theta_{ij}) + B_{ij} |V_i||V_j| \sin(\theta_{ij}) \right], \quad (14)$$

$$Q_{Gi} - Q_{Di} = \sum_{j=1}^{NB} \left[G_{ij} |V_i||V_j| \sin(\theta_{ij}) - B_{ij} |V_i||V_j| \cos(\theta_{ij}) \right], \quad (15)$$

where, i=1,…,NB.

2.2.2 System operating limit constraints

The system operating constraints are as follows.

(1) Generator constraints are,
- The limit on generators' voltage magnitude,

$$|V_{Gi}|^L \leq |V_{Gi}| \leq |V_{Gi}|^U \quad , \quad (16)$$

- The generators' real and reactive power operating limit,

$$P_{Gi}^L \leq P_{Gi} \leq P_{Gi}^U \quad (17)$$

$$Q_{Gi}^L \leq Q_{Gi} \leq Q_{Gi}^U \quad \text{, and} \quad (18)$$

i = 1,…,NG.

(2) Transformer tap-changing limit,

$$T_i^L \leq T_i \leq T_i^U \quad ,i = 1,...,NT \quad (19)$$

(3) The SVCs setting limits,

$$Q_{ci}^L \leq Q_{ci} \leq Q_{ci}^U \quad ,i = 1,...,NC \quad (20)$$

(4) Network operating limit constraints include,
- The limit on bus voltage magnitude,

$$|V_{Li}|^L \leq |V_{Li}| \leq |V_{Li}|^U \quad ,i = 1,...,NPQ \quad (21)$$

- The transmission lines and transformers loading limit,

$$|S_{Li}| \leq S_{Li}^U \quad ,i = 1,...,NL \quad (22)$$

3. STRATEGY FOR OBJECTIVE FUNCTIONS FUZZIFICATION

This section illustrates a multi-objective optimization technique using a fuzzy satisfactory approach which is proposed by Zimmermann [25]. With this approach, the optimization of MOOP can be solved by compromising trade-offs among all objectives. The MOOP is compared to a single-objective optimization problem by considering the solution at the edge of the fuzzy satisfactory functions, in this paper. The proposed FMOPF using PSO is categorized into:

(1) TSCM in Equation 9,
(2) APLM in Equation 11, and
(3) VMDM in Equation 13.

The objective functions in Equations 9 to 13 are used to formulate the fuzzy satisfactory functions (FSF) as shown in Figures 1 to 3.

In the fuzzification process, the MOOP is converted into FSF, μ_{TSC}, μ_{APL}, and μ_{VMD}, as shown in Figures 1 to 3, respectively. This process defines a FSFs associated with each objective because high value of each objective is given by a low FSF value. In the same manner, the best value for each objective is obtained by optimizing a single-objective. Meanwhile, the maximum objective value is determined by minimizing other objective functions.

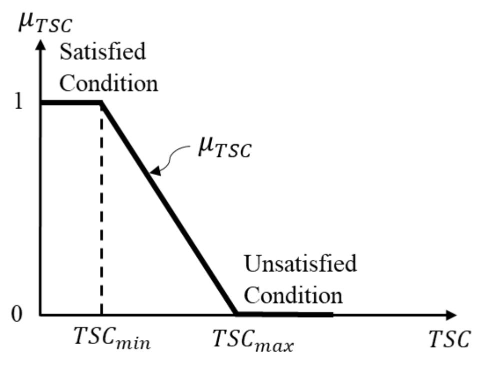

Fig. 1. FSF of TSC.

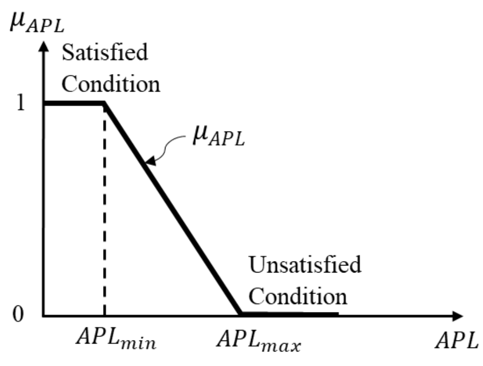

Fig. 2. FSF of APL.

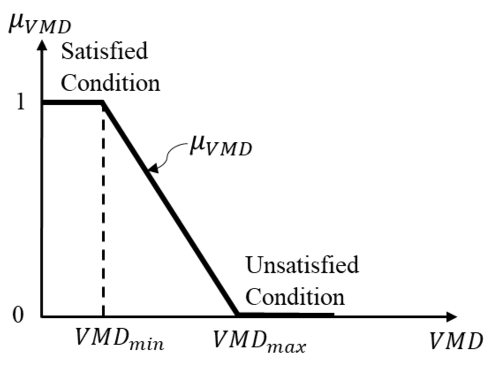

Fig. 3. FSF of VMD.

The FSF of the individual objective functions can be represented by Equations 23 to 25, for TSCM, APLM, and VMDM, respectively. A FSF can take any value in [0,1]. The FSF value of 1 is assigned to the minimum value for each objective. When the other objective provides that objective value is greater than the minimum value, the FSF is decreased to zero. Lastly, the multi-objective problem can be formulated as fuzzy maximization problem as Equation 26.

$$\mu_{TSC}=\begin{cases}1 & ,\text{for } TSC\le TSC_{\min}\\ \dfrac{-1}{TSC_{\max}-TSC_{\min}}\cdot TSC+\dfrac{TSC_{\max}}{TSC_{\max}-TSC_{\min}} & ,\text{for } TSC_{\min}\le TSC<TSC_{\max}\\ 0 & ,\text{for } TSC\ge TSC_{\max}\end{cases} \quad (23)$$

$$\mu_{APL}=\begin{cases}1 & ,\text{for } RPL\le RPL_{\min}\\ \dfrac{-1}{APL_{\max}-APL_{\min}}\cdot APL+\dfrac{APL_{\max}}{APL_{\max}-APL_{\min}} & ,\text{for } APL_{\min}\le APL<APL_{\max}\\ 0 & ,\text{for } APL\ge APL_{\max}\end{cases} \quad (24)$$

$$\mu_{VMD}=\begin{cases}1 & ,\text{for } VMD\le VMD_{\min}\\ \dfrac{-1}{VMD_{\max}-VMD_{\min}}\cdot VMD+\dfrac{VMD_{\max}}{VMD_{\max}-VMD_{\min}} & ,\text{for } VMD_{\min}\le VMD<VMD_{\max}\\ 0 & ,\text{for } VMD\ge VMD_{\max}\end{cases} \quad (25)$$

$$\text{Maximize } \mu_T=\min\{\mu_{TSC},\mu_{APL},\mu_{VMD}\} \quad (26)$$

3.1 PSO based FMOPF

The PSO was proposed in 1995 [26], as one of the bio-inspired algorithms and it is a simple one to search for an optimal search in the solution space, like the motion of bird flocks. In the proposed PSO based FMOPF, the individual single-object for TSCM, APLM, and VMDM are solved, in order to obtain the FSF of TSCM, APLM, and VMDM.

The PSO population i for single-objective is

$$\mathbf{p_i}=[\mathbf{P_{Gi}},\ |\mathbf{V_{Gi}}|,\ \mathbf{T_i},\ \mathbf{X_{Ci}}]. \quad (27)$$

Then, velocity of particle m can be computed by,

$$v_m^{t+1}=wv_m^t+c_1r_1(pbest_m^t-\mathbf{p}_i^t)+c_2r_2(gbest^t-\mathbf{p}_m^t)\ . \quad (28)$$

The particle's position is, then, updated as,

$$\mathbf{p}_m^{t+1}=\mathbf{p}_m^t+v_m^{t+1}\ . \quad (29)$$

The standard parameters of PSO are used for investigation of this work. Therefore, w is reduced from 0.9 at the first iteration to 0.4 at the maximum iteration, and c1 and c2 are 2.00. The proposed, the individual objective, computational procedure is shown in Figure 4. For FMOPF, the FSF is used to obtain μ_T. The computational can be illustrated as Figure 5.

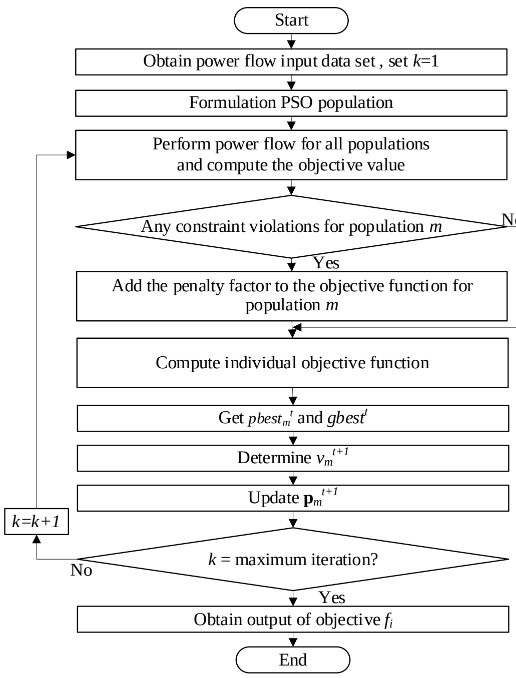

Fig. 4. Flow chart of the individual objective.

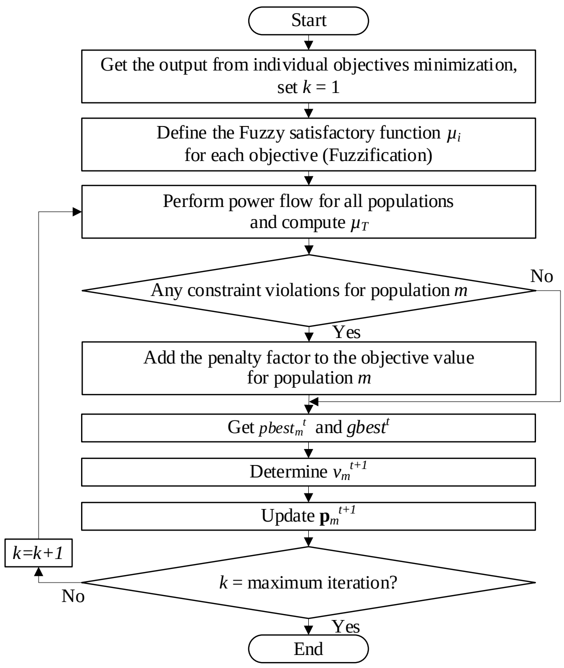

Fig. 5. Flow chart of the FMOPF using PSO.

4. SIMULATION RESULT AND DISCUSSION

In this section, the TSCM, APLM, VMDM are studied, which were tested on the standard and the modified IEEE 30-bus test systems, as shown in Figures 6 and 7, respectively. The system data is taken from [27] and [28]. The proposed FMOPF has been investigated in three cases study as follows.

4.1 Base Case for TSCM with Standard IEEE 30-bus Test System

For the base case, the control variables are as shown in Table 1. This case study investigates the performance of the proposed PSO-based OPF by comparing it to the widely-used standard case in [27].

Table 2 shows the results obtained from the convention deterministic method and the proposed method. The results showed that the proposed method can determine a lower TSC than the conventional deterministic method. Therefore, the proposed PSO-based OPF problem formulation can successfully minimize the TSC of the power system to satisfy system operating constraints. Further comparison result with the modified IEEE 30-bus test system is illustrated compared to more recent stochastic methods in Section 4.2.

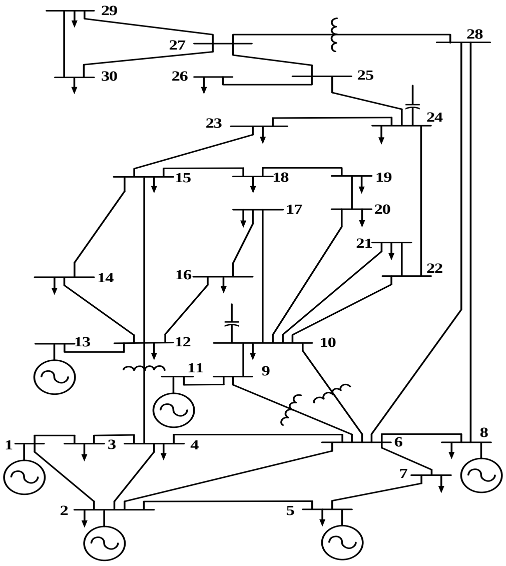

Fig. 6. The IEEE 30 buses system [27].

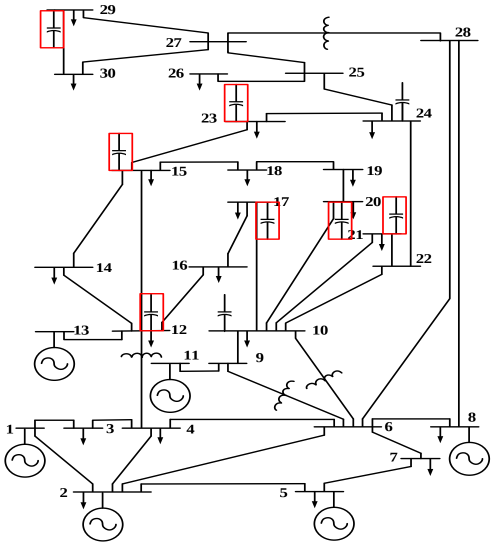

Fig. 7. The modified IEEE 30-bus test system [28].

Table 1. The control variables of standard case.

Control Variables	Number	At bus number
Real power generations	5	2, 5, 8, 11, 13
Generators' voltage magnitudes	6	1 (slack), 2, 5, 8, 11, 13
Transformer tap-changes	4	6-9, 6-10, 4-12, 27-28
SVCs' setting values	2	10, 24

Table 2. Comparison results of the IEEE 30-bus test system for TSCM.

Control Variables	Deterministic method	Proposed method
Power Generation (P_{Gi}) at Bus (MW)		
2	48.84	48.63
5	21.51	21.30
8	22.15	21.18
11	12.14	11.94
13	12.00	12.00
Generator Voltage ($\|Vi\|$) Magnitude at Bus (p.u.)		
1	1.05	1.10
2	1.04	1.09
5	1.01	1.06
8	1.02	1.07
11	1.09	1.10
13	1.09	1.10
Transformer Tap-Changing (T_{i-j}) between Buses		
6-9	1.00	1.04
6-10	0.96	0.94
4-12	1.00	0.99
28-27	0.94	0.96
SVC Reactance Values (X_{Ci}) at Bus (p.u.)		
10	-5.26	-5.00
24	-25.00	-20.00
TSC ($/h.)	802.400	799.430

4.2 The Single-Objective with Modified IEEE 30-bus Test System

The control variables of the modified IEEE 30-bus test system are shown in Table 3. The TSCM sing objective solution has been carried out and investigated compared to the enhanced genetic algorithm (EGA) method [29], BHBO method [30], and enhanced genetic algorithm-decoupled quadratic load flow (EGA-DQLF) method [31], as shown in Table 4.

From Table 4, the EGA method resulted in the highest TSC of 802.06 \$/h. Meanwhile, the BHBO and EGA-DQLF methods can provide the lower TSC at 799.922 and 799.56 \$/h, respectively. However, the TSC obtained by the proposed problem formulation is the lowest among all other methods. Therefore, the proposed method is potentially competitive with other existing stochastic methods for TSC minimization.

Table 3. The control variables of standard case.

Control Variables	Number	At bus number
Real power generations	5	2, 5, 8, 11, 13
Generators' voltage magnitudes	6	1 (slack), 2, 5, 8, 11, 13
Transformer tap-changes	4	6-9, 6-10, 4-12, 27-28
SVCs' setting values	9	10, 12, 15, 17, 20, 21, 22, 23, 24

Table 4. Comparison results of the modified IEEE 30-bus test system for TSCM.

Control Variables	EGA [29]	BHBO [30]	EGA-DQLF [31]	Proposed method
Power Generation (P_{Gi}) at Bus (MW)				
2	48.75	48.35	48.11	48.84
5	21.44	21.53	21.28	21.36
8	21.95	20.02	20.93	20.93
11	12.42	13.42	12.50	11.91
13	12.02	13.41	12.00	12.00
Generator Voltage ($\|V_i\|$) Magnitude at Bus (p.u.)				
1	1.05	1.10	1.10	1.10
2	1.04	1.08	1.08	1.09
5	1.01	1.05	1.05	1.06
8	1.01	1.06	1.06	1.07
11	1.08	1.08	1.10	1.04
13	1.07	1.07	1.09	1.07
Transformer Tap-Changing (Ti-j) between Buses				
6-9	1.01	1.02	0.95	1.08
6-10	0.95	1.00	1.04	0.99
4-12	1.00	1.03	1.00	1.05
28-27	0.96	1.00	0.98	1.04
SVC Reactance Values (X_{Ci}) at Bus (p.u.)				
10	-20.00	-33.23	-25.00	-18.02
12	-20.00	-33.69	-50.00	-29.56
15	-33.33	-28.94	-20.00	-34.91
17	-20.00	-28.16	-20.00	-15.66
20	-20.00	-40.84	-50.00	-45.00
21	-20.00	-36.03	-25.00	-9.42
23	-25.00	-35.74	-25.00	-44.99
24	-20.00	-29.52	-33.33	-15.65
29	-33.33	-37.21	-100.00	-44.99
TSC(\$/h.)	802.060	799.922	799.560	799.3862

4.3 The FMOPF with Modified IEEE 30-bus Test System

The proposed FMOPF for trading-off among TSCM, APLM, and VMDM had been investigated in this case study. This case study was done by the input data as in Table 3. To further verify the reliability of the proposed method, 20 trials for TSCM, APLM, VMDM, and μ_T of FMOPF have been performed, as shown in Table 5. It is seen that the results from several trials guarantee the reliability to get the feasible solution of the proposed method. Figures 8 to 11 showed the convergence behavior of the TSCM, APLM, VMDM, and μ_T of FMOPF, respectively. μT is the maximum FSF value among the minimum values of μ_{TSC}, μ_{APL}, and μ_{VMD}. Note that the minimization of $-\mu_T$ is solved for μ_T maximization.

Table 5. The results from 20 trials.

	Best	Avg.	Worst
TSCM ($/h.)	799.386	799.512	800.539
APLM (p.u.)	2.966	2.984	3.076
VMDM (p.u.)	0.081	0.089	0.141
μ_T of FMOPF	0.834	0.685	0.563

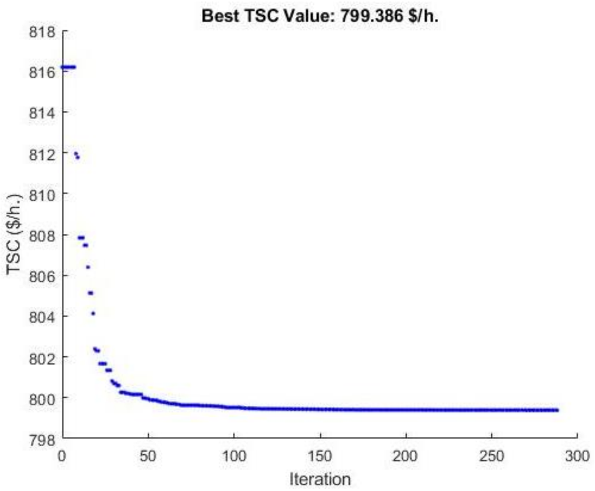

Fig. 8. The convergence behavior of TSCM.

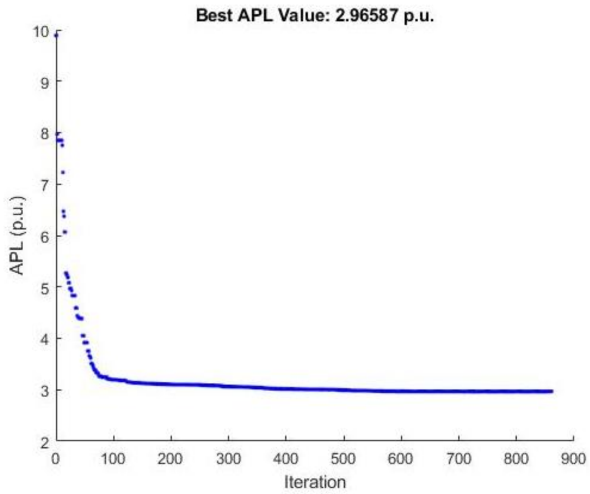

Fig. 9. The convergence behavior of APLM.

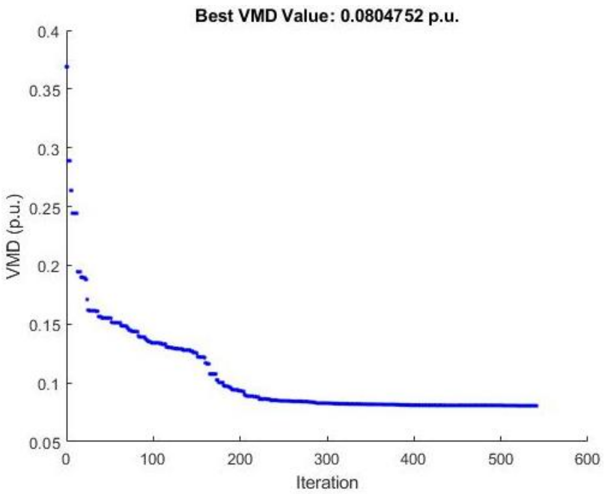

Fig. 10. The convergence behavior of VMDM.

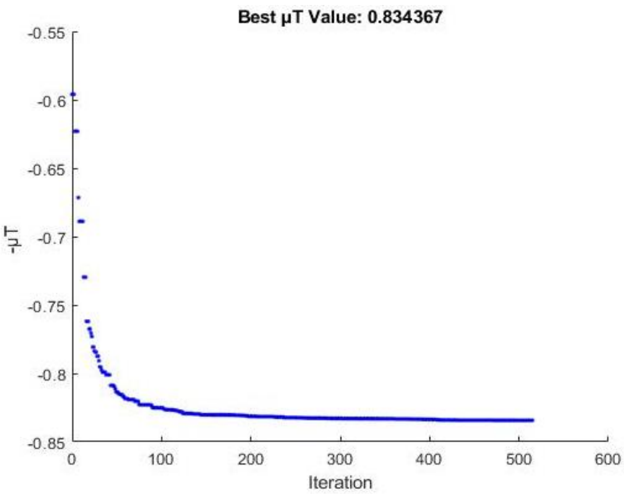

Fig. 11. The convergence behavior of μT of FMOPF.

The results of individual objectives and FMOPF are shown in Table 6. In FMOPF overview, it is obvious that when minimizing an individual single-objective can result in a higher solution for other objectives. The minimum TSC obtained from the proposed method is 799.386 $/h. Under this condition, the APL and VMD are 8.718 p.u. and 0.807 p.u., respectively. Meanwhile, when minimizing APL by APLM, the lowest value of APL is 2.966 p.u. However, the minimum APL condition is lead to the highest solution of TSC of 967.342 $/h. Similarly, the lowest VDM condition is lead to the higher value of TSC and APL at 929.577 $/h and 8.751 p.u.

To obtain a fair comparison with the PPSOGSA method [32], the simulations were tested under the same system data and control variables. A comparison of the proposed FMOPF and PPSOGSA method showed that the FMOPF yielded the results for the individual objective, including TSCM, ALPM, and VMDM, better than the results of the PPSOGSA method, as shown in Table 6. However, the performance of the system is significantly improved by simultaneous minimization of

TSC, APL, and VMD. Therefore, the cooperative solution among individual objectives may gain benefit to the system depending on the operator's requirement. When solving the MOOP using the proposed FMOPF for this case, the soft computational bargain between the contradiction objectives can be obtained. It is shown that a slightly increasing in TSC can decrease the VMD from 0.807 to 0.221 p.u. Simultaneously, the APL is reduced from 8.718 to 6.802 p.u. As a result, the proposed FMOPF can compromise among TSCM, APLM, and VMDM, under the fuzzy trade-off concept. Meanwhile, the PPSOGSA method uses the weighted sum method to solve the MOOP.

Table 6. Comparison results of the modified IEEE 30-bus test system for MOOP.

Control Variables	TSCM		APLM		VMDM		MOOP	
	PPSOGSA [32]	FMOPF	PPSOGSA [32]	FMOPF	PPSOGSA [32]	FMOPF	PPSOGSA [32]	FMOPF
Power Generation (P_{Gi}) at Bus (MW)								
2	48.58	48.84	80.00	80.00	49.04	80.00	52.66	46.40
5	21.37	21.36	50.00	50.00	44.74	49.97	31.73	36.64
8	21.44	20.93	35.00	35.00	18.41	35.00	34.94	34.94
11	11.94	11.91	30.00	30.00	24.13	10.11	25.28	17.20
13	12.00	12.00	40.00	40.00	14.50	29.80	20.38	16.17
Generator Voltage ($\|V_i\|$) Magnitude at Bus (p.u.)								
1	1.08	1.10	1.06	1.10	1.01	0.99	1.03	1.03
2	1.07	1.09	1.06	1.10	1.00	1.05	1.02	1.02
5	1.03	1.06	1.04	1.08	1.02	1.02	1.00	0.99
8	1.04	1.07	1.04	1.09	1.01	0.99	1.01	1.00
11	1.09	1.04	1.06	1.03	1.00	1.04	1.01	1.10
13	1.04	1.07	1.05	1.06	1.02	0.96	1.01	1.02
Transformer Tap-Changing ($T_{i\text{-}j}$) between Buses								
6-9	1.02	1.08	1.02	1.10	1.02	1.05	1.03	1.02
6-10	0.95	0.99	0.94	0.97	0.90	1.08	0.91	1.04
4-12	0.96	1.05	0.99	1.05	1.01	0.94	0.98	0.98
28-27	0.98	1.04	0.98	1.05	0.96	0.99	0.97	0.98
SVC Reactance Values (X_{Ci}) at Bus (p.u.)								
10	-1.39	-18.02	-0.26	-45.00	-0.22	-20.03	-0.20	-43.29
12	-0.72	-29.56	-0.47	-29.31	-0.28	-23.77	-0.95	-24.25
15	-0.22	-34.91	-0.21	-28.98	-0.20	-45.00	-0.21	-44.67
17	-0.20	-15.66	-0.20	-15.77	-3.08	-13.63	-1.40	-42.37
20	-0.25	-45.00	-0.22	-45.00	-0.20	-44.20	-0.20	-45.00
21	-0.20	-9.42	-0.20	-9.59	-0.20	-7.41	-0.20	-22.24
23	-0.26	-44.99	-0.29	-45.00	-0.20	-26.95	-0.20	-43.25
24	-0.20	-15.65	-0.20	-14.14	-0.20	-8.72	-0.20	-44.39
29	-0.30	-44.99	-0.37	-45.00	-0.77	-43.30	-0.34	-45.00
TSC ($/h.)	800.528	799.386	967.669	967.342	849.613	929.577	829.598	827.206
APL (p.u.)	9.027	8.718	3.103	2.966	7.420	8.751	6.110	6.802
VMD (p.u.)	0.911	0.807	0.891	0.888	0.090	0.081	0.110	0.221

5. CONCLUSION

This paper proposed the FMOPF formulation with various control variables using PSO. The proposed method can successfully provide the optimal operating condition of the active power generation, the generator voltage magnitudes, the transformers tap changings, and the SVCs setting values. The considered objectives are TSCM, APLM, and VMDM. The fuzzy concept is applied to solve the MOOP, tested on the original and the modified IEEE 30-bus test system. The proposed FMOPF has the ability and good performance to obtain the compromised solution among conflictual objectives.

NOMENCLATURE

$\|S_{Li}\|$	the MVA flow of line i (MVA)
$\|V_{Gi}\|$	the voltage magnitude of generator at bus i (p.u.).
$\|V_i\|$	the voltage magnitudes at bus i (p.u.).
$\|V_i^{ref}\|$	the reference value of the voltage magnitude at bus i.
$\|V_j\|$	the voltage magnitudes at bus j (p.u.).
$\|V_{Li}\|$	the voltage magnitude at load bus i (p.u.).
μ_{APL}	the fuzzy satisfaction function of active power loss.

μ_T	the fuzzy satisfaction function.
μ_{TSC}	the fuzzy satisfaction function of total system cost.
μ_{VMD}	the fuzzy satisfaction function of voltage magnitude deviation.
a_i, b_i, c_i	the cost coefficients parameters of generator *i*.
APL	the active power loss (p.u.).
APL_{max}	the maximum acceptable active power loss obtained by TSCM and VDM.
APL_{min}	the minimum active power loss obtained by RPLM.
B_{ij}	the imaginary of admittance between buses *i* and *j*.
f_i	the objective function to be optimize.
g	the equality constraints representing nonlinear power flow equations.
G_{ij}	the real parts of admittance between buses *i* and *j*.
$g_{L,ij}$	the conductance of line *L* between buses *i* and *j*.
h	the system operating constraints.
NB	the buses total number.
NC	the shunt compensators total number.
NG	the generators total number.
NL	the branches total number.
N_{obj}	the objectives total number.
NPQ	the PQ buses total number.
NT	the transformers total number.
NTL	the transmission line total number.
P_{Di}	the real power load demand at bus *i* (MW, p.u.).
P_{Gi}	the real power generation at bus *i* (MW, p.u.).
Q_{Ci}	the shunt VAR compensator (p.u.).
T_i	the transformer tap changing (p.u.).
TSC	the total system cost ($/h.).
TSC_{max}	the maximum acceptable total system cost obtained by RPLM and VDM.
TSC_{min}	the minimum total system cost obtained by TSCM.
$\boldsymbol{u}$	the column vector of independent control variables.
VD	the voltage deviation (p.u.).
VD_{max}	the maximum acceptable voltage deviation obtained by TSCM and RPLM.
VD_{min}	the minimum voltage deviation obtained by VDM.
$\boldsymbol{x}$	the vector of dependent variables.
θ_{ij}	the voltage angles between buses *i* and *j* (radian).

Superscript

L	lower limit.
U	upper limit.

REFERENCES

[1] Carpentier J., 1962 Contribution á l'étude du dispatching économique. *Bulletin de la Société Française des Électriciens*3: 431-447.

[2] Lesieutre. B.C., 2005. Convexity of the set of feasible injections and revenue adequacy in FTR markets. *IEEE Transactions on Power Systems* 20: 1790-1798.

[3] Molzahn D.K., 2018. Identifying and characterizing non-convexities in feasible spaces of optimal power flow problems. *IEEE Transactions on Circuits and Systems II: Express Briefs* 65(5): 672-676.

[4] Wu D. and B.C. Lesieutre. 2018. A Deterministic method to identify multiple local extrema for the AC optimal power flow problem. *IEEE Transactions on Power Systems* 33(1): 654-668.

[5] Nguyen T.T., 2019. A high-performance social spider optimization algorithm for optimal power flow solution with single objective optimization. *Energy* 171(C): 218-240.

[6] Bakirtzis A.G., Biskas N.P., Zoumas E.C, and Petrids V., 2002 Optimal power flow by enhanced genetic algorithm. *IEEE Transactions on Power Systems* 17(2): 229-236.

[7] Abido M.A., 2002. Optimal power flow using tabu search algorithm, *Electric Power Components and Systems* 30(5): 469-483.

[8] Bouchekara H.R.E.H., 2014. Optimal power flow using black-hole-based optimization approach, *Applied Soft Computing* 24(C): 879-888.

[9] Ladumor D.P., Bhesdadiya R.H., Trivedi I.N., and Jangir P., 2017. Optimal power flow problem solution with SVC using meta-heuristic algorithm In the *Proceedings of the 3rd International Conference on Advances in Electrical, Electronics, Information, Communication and Bioinformatics (AEEICB17)*, 27-28 February 2017, Chennai, India.

[10] Li S., Gong W., Wang L., Yah X., and Hu C., 2020. Optimal power flow by means of improved adaptive differential evolution. *Energy* 198: 117314.

[11] Abido M.A., 2002. Optimal power flow using particle swarm optimization. *Electrical Power and Energy Systems* 24(7): 563-571.

[12] Kumar C. and C.P. Raju. 2012. Constrained optimal power flow using particle swarm optimization. *International Journal of Emerging Technology and Advanced Engineering* 2(2): 235-241.

[13] Turkay B.E. and R.I. Cabadag. 2013. Optimal power flow solution using particle swarm optimization algorithm, *EuroCon* 2013: 1418-1424.

[14] Le L.D., Ho L.D, Polprasert J., Ongsakul W., Vo D.N., and Le D.A, 2014. Stochastic weight trade-off particle swarm optimization for optimal power flow. *Journal of Automation and Control Engineering* 2(1): 31-37.

[15] Sivasubramani S. and K.S. Swarup. 2011. Multi-

objective harmony search algorithm for optimal power flow problem. *Electrical Power and Energy Systems* 33(3): 745-752.

[16] Deb K., 2001. *Multi-Objective Optimization Using Evolutionary Algorithms*. John Wiley & Sons, Inc. 605 3rd Avenue, New York, NY, United States.

[17] Ramesh V.C. and X. Li. 1997. A fuzzy multiobjective approach to contingency constrained OPF. *IEEE Transactions on Power Systems* 12(3): 1348-1354.

[18] Khorsandi A., Hosseiniana S.H., and Ghazanfari A., 2013. Modified artificial bee colony algorithm based on fuzzy multi-objective technique for optimal power flow problem. *Electric Power Systems Research* 95: 206-213.

[19] Liang R.H. and Y.Y. Hsu. 1994. Fuzzy linear programming: an application to hydroelectric generation scheduling. *IEEE Proceedings-Generation, Transmission and Distribution* 141(6): 568-574.

[20] Chayakulkheeree K., 2011. Unified multi-objective optimal power flow considering emissions with fuzzy network and generators ramp-rate constraints In the *Proceedings of the 8th Electrical Engineering/Electronics, Computer, Telecommunications, and Information Technology (ECTI)*, 17-19 May 2011, Khon Kaen, Thailand.

[21] Khamees A.K., Abdelaziz A.Y., Eskaros M.R., Alhelou H.H., and Attia M.A., 2021. stochastic modeling for wind energy and multi-objective optimal power flow by novel meta-heuristic method. *IEEE Access* 9: 158353-158366.

[22] Shaheen A.M., Farrag S.M., and El-Sehiemy R.A., 2017. MOPF solution methodology. *IET Generation, Transmission and Distribution* 11(2): 570-581.

[23] Naderia E., Pourakbari-Kasmaeib M., Cernac F.V, and Lehtonen M., 2021. A novel hybrid self-adaptive heuristic algorithm to handle single- and multi-objective optimal power flow problems. *International Journal of Electrical Power & Energy Systems* 125.

[24] Kahraman H.T., Akbel M., and Duman S., 2022. Optimization of optimal power flow problem using multi-objective manta ray foraging optimizer. *Applied Soft Computing* 116: 108334.

[25] Zimmermann H.-J., 1987. *Fuzzy Sets. Decision Making, and Expert Systems*: Kluwer Academic Publishers, Boston, USA.

[26] Kennedy J., and R. Eberhart. 1995. Particle Swarm Optimization. *Proceedings of the IEEE International Conference on Neural Networks* 4: 1942-1948.

[27] Alsac O. and B. Stott. 1974. Optimal load flow with steady state security. *IEEE Transactions on Power Apparatus and Systems*. PAS-93:745-751.

[28] Sivasubramani S. and K.S. Swarup. 2011. Multi-objective harmony search algorithm for optimal power flow problem. *International Journal of Electrical Power & Energy Systems* 33(3): 745-75.

[29] Bakirtzis A.G., Biskas N.P., Zoumas C.E., and Petrids V., 2002. Optimal power flow by enhanced genetic algorithm. *IEEE Transactions on Power Systems* 17: 229-236.

[30] Bouchekara H.R.E.H., 2014. Optimal power flow using black-hole-based optimization approach. *Applied Soft Computing* 24: 879-888.

[31] Kumari M.S. and S. Maheswarapu. 2010. Enhanced genetic algorithm-based computation technique for multi-objective optimal power flow solution. *Electrical Power and Energy Systems* 32(6): 736-742.

[32] Ullah Z.,Wang S., Radosavlievic J., and Lai J., 2019. A Solution to the optimal power flow problem considering WT and PV generation *IEEE Access* 7: 46763-46772.